Synthesis of Oxide-Free InP Quantum Dots: Surface Control and H2-Assisted Growth

Edwin A Baquero, Héloïse Virieux, Robert Swain, Angélique Gillet, Arnaud Cros-Gagneux, Yannick Coppel, Bruno Chaudret, Céline Nayral, Fabien Delpech

Synthesis of Oxide-Free InP Quantum Dots: Surface Control and H_2-Assisted Growth

Edwin A. Baquero,[a,b] Héloïse Virieux,[a] Robert A. Swain,[a] Angélique Gillet,[a] Arnaud Cros-Gagneux,[a] Yannick Coppel,[c] Bruno Chaudret,[a] Céline Nayral,[a]* and Fabien Delpech[a]*

[a] LPCNO, Université de Toulouse, CNRS, INSA, UPS, 135 avenue de Rangueil, 31077 Toulouse, France.

[b] Departamento de Química, Facultad de Ciencias, Universidad Nacional de Colombia Sede Bogotá, Carrera 30 No. 45-03, 111321 Bogotá, Colombia

[c] Laboratoire de Chimie de Coordination, UPR-CNRS 8241, 205 route de Narbonne, 31077 Toulouse Cedex, France.

Supporting Information Placeholder

ABSTRACT: Control over particle surfaces and interfaces is a principal requirement to fully take advantage of semiconducting Quantum Dot (QDs) properties. In the case of indium phosphide, the sensitivity of the material to water renders it challenging to synthesize oxide-free particles. We demonstrate the ability to achieve complete control over the surface by developing synthetic strategies based on a novel reactive indium precursor, tris(N,N'-diisopropylacetamidinato) indium(III). This complex permits the synthesis of InP QDs at temperatures as low as 150°C with no inherent surface oxidation. At higher temperatures (230°C), the concomitant use of an H_2 atmosphere yields oxide-free InP QDs. The prevention of such an amorphous oxide layer provides a clean surface suitable for subsequent growth. An extensive solid-state ^2H NMR spectroscopy study demonstrates an unprecedented H_2 bond dissociation at the QD surface yielding QDs-H species and in so doing protecting the surface from oxidation.

At the nanoscale, the role of the particle surface is predominant for the chemical (solubility, colloidal stability, catalytic activity…) and physical (optical, magnetic, transport…) properties. Understanding the surface properties of nanoparticles is thus key to controlling their features. The surfaces of several semiconductor nanocrystals (Quantum Dots, QDs) have been investigated by many, leading to a substantial amount of knowledge and control.[1-4] This has opened the door to great achievements in many scientific disciplines, as exemplified by the use of these materials as bio-labels, lasers, light-emitting diodes (LEDs), and solar cells.[1-5] However, most such advancements have been achieved for toxic Cd- and Pb-based systems, while others, such as III-V semiconductors (in particular InP),[6-7] have not been as thoroughly studied. Indeed, the more covalent nature of the In-P solid and its high sensitivity toward oxidation account for the complexity of controlling both the InP surface chemistry and, in the case of core/shell systems, the shelling interface.[8-9] We and others have demonstrated the sensitivity of these materials to the water present in solution either as a reactant impurity or as a by-product generated under the high-temperature conditions of currently reported syntheses.[8-12] This results in the formation of oxide and hydroxide species, which dramatically and irreversibly alter the surface. It is important to note that the presence of water in the InP synthesis medium is not an exception but rather the general case. Most procedures are predicated on the use of indium carboxylate precursors and/or other oxygen-containing ligands at high temperatures (>188°C). Carboxylic acids, one such stabilizing agent, produce water as a co-product of decarboxylative coupling in this temperature range,[8-9] leading to unexpected and unwanted effects,[8-9,11-12] most notably the inhibition of further particle growth. This phenomenon serves as an immense obstacle to the accurate study of QD growth mechanisms, as it renders impossible the independent isolation and investigation of other parameters. The true effect of acid concentration on particle growth, for example, cannot be satisfactorily described while the concentration of water varies simultaneously.[6-7] Moreover, the pivotal (and sometimes detrimental) effect of water has been demonstrated even in the case of materials considered to be largely resistant. For instance, in both PbS QDs and CdSe nanoplatelet systems, water and hydroxide ligands alter the surface energy of specific planes.[13-14] Likewise, water is suspected to engender deterioration of the optical and electrical properties of PbSe and PbS QDs-based films.[15-16]

Herein, we address the issue of InP QD surface chemistry control, and in particular, the prevention of surface oxidation/hydroxylation, even when in the presence of O-containing ligands and water. We describe two alternative approaches based on a novel indium precursor: tris(N,N'-diisopropylacetamidinato) indium(III). Interestingly, while indium amidinate complexes have been known for a long time,[17] they have only very recently been used as reagents for CVD and ALD growth of indium-based materials.[18-19] The use of this particular indium amidinate complex in our colloidal synthesis produces particles completely devoid of oxides, allowing them to grow to larger diameters. The mechanism of protection from oxidation at 150°C (under argon) and at 230°C (under dihydrogen) are described. In the latter case, an unprecedented H_2 bond dissociation at the QD surface is demonstrated by ^2H Magic Angle Spinning (MAS) NMR.

The general consensus suggests that the elevated temperatures necessary to standard InP syntheses are a direct consequence of the high stability of the indium precursors.[7] Hoping to prepare InP QDs under softer conditions, a more reactive indium precursor featuring In–N bonds (186 kJ/mol) instead of In–O bonds (320 kJ/mol for the common precursor indium acetate) was selected. We successfully prepared InP QDs under argon at temperatures as low as 150°C by adding the tris(trimethylsilylphosphine ($P(TMS)_3$) to a solution containing the indium precursor as well as hexadecylamine (HDA) and palmitic acid (PA) in a 1:3 ratio, both of which play only the role of ligands (**1** in Scheme 1).

Scheme 1. Synthesis of InP QDs based on the use of a more reactive In precursor. PA = Palmitic Acid; HDA = Hexadecylamine

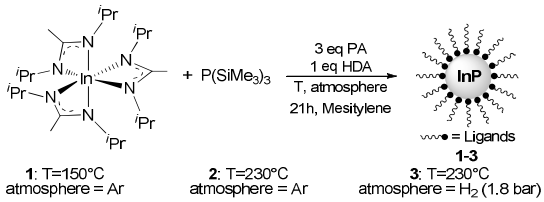

Transmission electron microscopy (TEM) images of **1** (Figure S1a) indicate the presence of monodisperse spherical InP QDs (2.0 ± 0.3 nm). X-ray diffraction (XRD) analysis reveals that the particles have a zinc blende structure (Figure S1b), and the UV-Vis spectrum shows an absorption peak at 530 nm (Figure S1c). The replacement of indium carboxylate with indium amidinate thus allows us to significantly decrease the required temperature for the preparation of high-quality InP QDs. In all previously published syntheses, temperatures higher than 160°C are required.[6] Interestingly, both the ^{31}P Hahn-echo and the ^{1}H-^{31}P Cross-Polarization (CP) Magic Angle Spinning (MAS) solid state NMR spectra of this sample (Figure S5) show only one resonance (located at δ -200 ppm). This high-field signal is assigned to nanoparticulate metal phosphides.[8-9] No other signals are present in the spectrum, meaning that there are no surface oxides (typically found at chemical shifts between 50 and 0 ppm).[8-9] Prior to this study, whenever surfaces have been precisely and rigorously characterized by XPS or ^{31}P NMR, surface oxidation has been ubiquitously implicated on particles stabilized by oxygen-containing ligands.[20-23]

Evidence of coordination of PA and HDA ligands to the QD surface is provided by the ^{1}H–^{13}C (CP) MAS spectrum (top in Figure S7), the carboxylate resonance appears at δ 182 ppm and the alpha-CH_2 group of HDA at δ 42 ppm. Two additional broad peaks at 162 and 172 ppm are assigned to the resonances of the amidinate sp^2 carbon and to the acyl group of the amide, respectively. The intensity of these resonances are significantly decreased in the ^{13}C Direct Polarization (DP) spectrum (bottom in Figure S7), an effect of long relaxation times which are due to the ligand rigidity at the QD surface. In contrast, the signal intensity of the terminal methyl group (δ 15 ppm) is enhanced due to its increased mobility. Firstly, this demonstrates the complexity of the surface of these QDs, which possess a coordination sphere consisting of at least four types of molecules. Secondly and more importantly, we also note the formation of amide, which results from a reaction between acid and amine, and is accompanied by *in-situ* water formation.[24-25] However, despite the presence of water, no oxidation occurs at the InP QD surface (Figure S5), suggesting that at temperatures as low as 150°C, water cannot effectively diffuse through the layer of the coordination sphere. In order to grow larger particles, the reaction was performed at 230°C (**2** in Scheme 1). By TEM we observe spherical QDs with a diameter of 4.1 ± 0.4 nm (Figure S2a), indicating that the temperature increase favors growth. This growth is also apparent in the UV-Vis spectrum (Figure S2c), which shows a red-shifted absorption peak with respect to that of **1** (570 vs 530 nm). Increasing the temperature also results in some modifications to the QD coordination sphere, as can be seen in the MAS ^{13}C spectra (Figure S9). The characteristic amidinate peak at 162 ppm is no longer present, while a significant increase in the intensity of the resonance of amide relative to that of the carboxylate is observed in the ^{1}H–^{13}C CP MAS spectrum (top in Figure S9). This suggests that conversion of carboxylate proceeds further into amide at 230°C than at 150°C. In contrast to our synthesis at 150°C, and as has been observed in previous InP syntheses,[10] the oxidation of the surface occurs concurrently with the production of amide and water: hence, in addition to the broad and high-field resonance of metal phosphides at -185 ppm, we observe two more phosphorus environments (identified as $InPO_4$ and $InPO_3$)[8-9] as evidenced by the resonances at δ 2 and 28 ppm in the ^{31}P Hahn-echo MAS NMR spectrum (Figure 1a). This sequence also allows quantification (the relative ratio is 85:7:8 respectively) that 15% of the P atoms of the QDs are oxidized.

Figure 1. ^{31}P Hahn-echo MAS NMR spectrum of (a) InP QDs **2** (spinning rate 16 kHz), (b) InP QDs **3** (spinning rate 18 kHz)

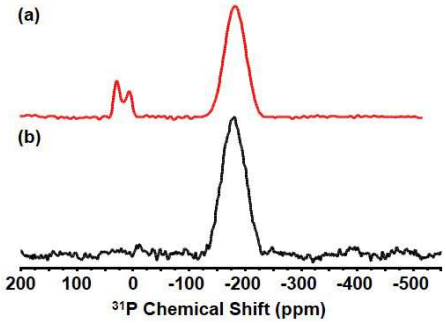

In an effort to avoid surface oxidation, the same procedure was carried out at 230°C under an H_2 atmosphere (1.8 bar) (**3** in Scheme 1). In the field of III-V semiconductor technology, the use of hydrogen plasmas was identified long ago as a practical method for passivating defects and removing surface carbon contaminations and native oxides leaving a clean and well-ordered surface for epitaxial growth.[26] In contrast, hydrogenation via an H_2 atmosphere was identified as being inefficient.[27] In the matter at hand, however, dihydrogen treatment proves to be a highly valuable upgrade. TEM images show QDs of 4.5 ± 0.5 nm (Figure S3a) indicating that the reductive atmosphere favors the growth of the QDs. This observation is confirmed in the UV-Vis spectrum as the absorption peak appears at 610 nm (Figure S3c), significantly red-shifted to that of sample **2** (570 nm). As expected, XRD measurements indicate that the particles are zinc blende structure (Figure S3b). The H_2 atmosphere does not inhibit the condensation reaction between acid and amine, as the C=O amide resonance is again visible at δ 171.8 ppm in the ^{1}H-^{13}C CP-MAS NMR spectrum (Figure S12). However, the ^{1}H-^{31}P CP-MAS and the ^{31}P MAS NMR spectra show only one resonance at δ -190 ppm (Figures 1b and S10) demonstrating that under these conditions, surface oxidation is prevented. While these uncoated QDs **2** and **3** do not display any photoluminescence, shelling with ZnS using a previously reported procedure[28] (See Supporting Information for details) yields core/shell QDs emitting at 610 and 680 nm (Figures S20 and S22) with 13% and 33% quantum yields, both values taken respectively.

The two InP samples **2** (oxidized QDs) and **3** (non-oxidized QDs) also provide a unique opportunity to investigate the influence of the oxide layer on otherwise similar QD samples. As such, growing experiments were performed on freshly prepared InP samples **2** and **3** by adding (in the same relative stoichiometry) all starting materials several times (one-third of the initial amount used for the preparation of InP QDs in each addition). The reaction was monitored by TEM (Figures S17 and S18) and UV-Vis spectroscopy (Figure 2). Both techniques clearly demonstrate successful particle growth of sample **3**: in the UV-Vis spectrum (Figure 2b), the absorption peak redshifts with each successive addition (for an overall change from 600 to 680 nm), and TEM images indicate a final size of 6.7 nm, 50% larger than the initial 4.5 nm particles. The size distribution of the particles is un-

changed, but the morphology, spherical during the initial additions, becomes tetrahedral after the final addition (Figure S17). On the other hand, the growth is blocked for sample **2** (Figure 2a) after the 3rd addition with only a minimal overall size change (the absorption peak shifts from 570 to 600 nm and the particle diameter from 3.9 to 4.4 nm, Figure S18). This slight increase in size is possible because there remain some non-oxidized surface sites: By the ^{31}P MAS NMR spectrum, 15% of the P atoms are oxidized (for 3.9 nm QDs, ca. 28% of the total number of P atoms are expected to be surface atoms).[29] The substantial difference between samples **2** and **3** over the course of this growing experiment proves that surface oxides significantly hinder particle growth.

Figure 2. UV-Vis spectra of growth InP QDs from a) **2** and b) **3** (each addition corresponds to one-third amount of the initial amount of precursors and ligands used for the synthesis of either **2** or **3**)

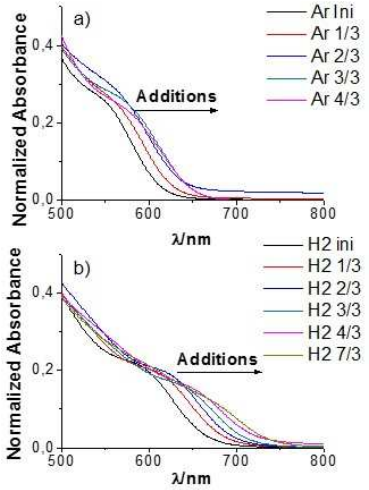

To elucidate the mechanism of surface protection against oxidation, InP QDs were synthesized under the same conditions as that of sample **3**, with D_2 (1.8 bar) used in place of H_2 (sample **4**, see Supporting Information for details). ^{2}H NMR spectroscopy has previously been identified as a useful tool to study the interaction of hydrogen with metal nanoparticles.[30-31] The lower gyromagnetic ratio of ^{2}H compared to ^{1}H results in decreased dipolar coupling and thus ^{2}H NMR spectra affords a narrower linewidth. As expected, **4** shows similar physical properties (shape, size, absorption peak and crystalline structure, Figure S4) and chemical composition (unoxidized surface, Figure S13 and amide formation, Figure S14) to its analogous particles synthesized under H_2 (**3**). The experimental and simulated ^{2}H solid-echo MAS NMR spectra of **4** are shown in Figure 3. A near-perfect fitting (Figure 3a) shows four signals, three of them presenting a significant quadrupolar coupling constant (C_Q): (i) δ_{iso} = 8.8(± 0.2) ppm (C_Q = 170(± 5) kHz), (ii) δ_{iso} = 3.1(± 0.3) ppm (C_Q = 145(± 15) kHz) and (iii) δ_{iso} = 2.0(± 0.3) ppm (C_Q = 95(± 15) kHz). The fourth contribution shows a Lorentzian shape without quadrupolar coupling at δ_{iso} = 1.1(± 0.1) ppm. The three components with quadrupolar coupling also appear in the ^{2}H-^{1}H CP-MAS experiment (Figure S15), indicating that they are in close proximity to ^{1}H nuclei and that their motion is restricted. The signal at ~8.8 ppm is attributed to deuterated amide in the N atom (e.g. –NDCO–), whereas the 3.1 and 2.1 signals are assigned to P–D species (respectively In_3PD and In_2PD_2). C_Q values provide valuable information about the mobility of the deuteron; smaller values correspond to increased mobility.[31] The amide resonances display the highest C_Q values as the consequence of tight coordination and steric hindrance. Considering the two types of P–D species, the smaller C_Q is attributed to the deuteron of In_2PD_2 consistent with the less-hindered environment relative to that of In_3PD. The last component at 1.1 ppm in ^{2}H solid-echo MAS NMR spectrum is not observed in the ^{2}H-^{1}H CP-MAS spectrum (Figure S15) due to its large mobility (which averages the C_Q to zero). This resonance can be assigned to the ND_2 moiety of residual mobile amine molecules. The deuterium is thus incorporated both at the surface of the QDs and in the coordinated ligands. A probable mechanism to account for these observations is the activation of gaseous deuterium onto the InP surface followed by H/D exchange in both the amide and the amine. We note that deuterium incorporation requires the presence of the InP QDs, as no signal could be observed in the ^{2}H solid-echo MAS spectrum of a mixture of PA/HDA alone in the same conditions (21h at 230°C, 1.8 bar D_2, Figure S16). These findings clearly support that H_2 (D_2) molecules are activated (dissociated) at the QDs surface yielding QD–H(D) bonds. While the formation of P–D bonds is unambiguously evidenced, the signature of In–D bonds is not apparent. This is not surprising, as extensive broadening is anticipated on account of both the wide distribution of chemical environments and (more importantly) the large quadrupole moment of indium nuclei (I=9/2).[32] This formation of QD–H surface species explains why InP QDs are not oxidized in the presence of H_2 despite the water-forming condensation reaction simultaneously occurring during the QDs synthesis.

Figure 3. (a) Experimental (blue) and simulated (red) ^{2}H solid-echo MAS spectrum of InP QDs **4** (spinning rate 8 kHz). (b, c, d) simulated spectra of the signal at 8.8, 3.1 and 2.0 ppm (e) Expanded view of the +10/-10 kHz area with full intensity and the simulated lorentzian signal at 1.1 ppm (in black). The simulated spectrum was slightly shifted to facilitate comparison.

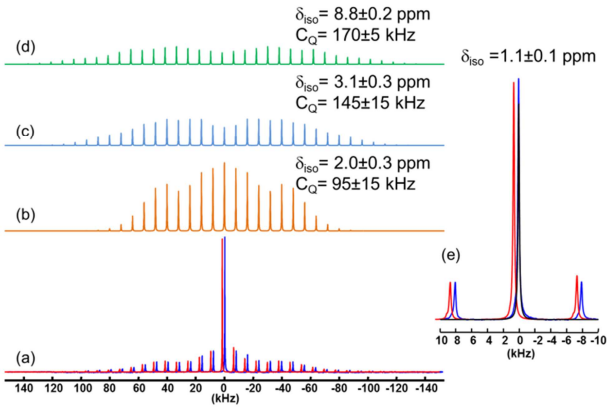

In conclusion, drawing on a profound understanding of InP QD surface chemistry, we have designed two novel approaches to overcome the ubiquitous surface alteration by O-containing ligands and by-products. We first demonstrate that the high energy indium precursor tris(N,N'-diisopropylacetamidinato) indium(III) is reactive at temperatures low enough (150°C) to prevent the oxidation of the resulting particles, despite the *in-situ* water formed as a by-product. Alternatively, at higher temperatures (230°C), when such an oxidation cannot be avoided under argon, we demonstrate the benefits of using an H_2 atmosphere. We show that H_2 dissociation occurs at the QD surface, ultimately protecting the particles from oxidation and leaving a clean surface suitable for subsequent growth. This opens the door for accurate study of the fundamental chemistry of these systems (growth mechanism, influence of the synthesis parameters…) but also of the physics of InP QDs, which is undoubtedly affected by the until-now unavoidable defects caused by amorphous surface oxides.

Moreover, our approach could be extended to various other semiconductor materials, further opening new perspectives – even for highly-characterized systems such as cadmium and lead chalcogenides.

ASSOCIATED CONTENT

Supporting Information

The Supporting Information is available free of charge on the ACS Publications website. Experimental section, TEM, UV-Vis, XRD and solid state NMR data of InP QDs **1**–**4**, and the ZnS-coated versions **5**–**6**.

AUTHOR INFORMATION

Corresponding Author

*E-mail cnayral@insa-toulouse.fr (C.N.) and fdelpech@insa-toulouse.fr (F.D.)

Notes

The authors declare no competing financial interests.

ACKNOWLEDGMENT

This work was supported by the Université Paul Sabatier, the Région Midi-Pyrénées, the CNRS, the Institut National des Sciences Appliquées of Toulouse, the European Commission for ERC Grant No. 694159 and the Agence Nationale pour la Recherche (Project ANR-13-IS10-0004-01). E. A. B. is grateful to Marie Curie Actions and Campus France for a PRESTIGE post-doc fellowship (FP7/2007–2013) under REA grant agreement no. PCOFUND-GA-2013-609102.

REFERENCES

(1) Hendricks, M. P.; Campos, M. P.; Cleveland, G. T.; Jen-La Plante, I.; Owen, J. S. A Tunable Library of Substituted Thiourea Precursors to Metal Sulfide Nanocrystals. *Science* **2015**, *348*, 1226-1230.

(2) Kovalenko, M. V.; Manna, L.; Cabot, A.; Hens, Z.; Talapin, D. V.; Kagan, C. R.; Klimov, V. I.; Rogach, A. L.; Reiss, P.; Milliron, D. J.; Guyot-Sionnnest, P.; Konstantatos, G.; Parak, W. J.; Hyeon, T.; Korgel, B. A.; Murray, C. B.; Heiss, W. Prospects of Nanoscience with Nanocrystals. *ACS Nano* **2015**, *9*, 1012-1057.

(3) Boles, M. A.; Ling, D.; Hyeon, T.; Talapin, D. V. The Surface Science of Nanocrystals. *Nat. Mater.* **2016**, *15*, 141-153.

(4) Hens, Z.; Martins, J. C. A Solution NMR Toolbox for Characterizing the Surface Chemistry of Colloidal Nanocrystals *Chem. Mater.* **2013**, *25*, 1211-1221.

(5) Talapin, D. V.; Lee, J.-S.; Kovalenko, M. V.; Shevchenko, E. V. Prospects of Colloidal Nanocrystals for Electronic and Optoelectronic Applications. *Chem. Rev.* **2010**, *110*, 389-458.

(6) Gary, D. C.; Terban, M. W.; Billinge, S. J. L.; Cossairt, B. M. Two-Step Nucleation and Growth of InP Quantum Dots via Magic-Sized Cluster Intermediates. *Chem. Mater.* **2015**, *27*, 1432-1441.

(7) Tamang, S.; Lincheneau, C.; Hermans, Y.; Jeong, S.; Reiss, P. Chemistry of InP Nanocrystal Syntheses. *Chem. Mater.* **2016**, *28*, 2491-2506.

(8) Cros-Gagneux, A.; Delpech, F.; Nayral, C.; Cornejo, A.; Coppel, Y.; Chaudret, B. Surface Chemistry of InP Quantum Dots: A Comprehensive Study. *J. Am. Chem. Soc.* **2010**, *132*, 18147-18157.

(9) Virieux, H.; Le Troedec, M.; Cros-Gagneux, A.; Ojo, W.-S.; Delpech, F.; Nayral, C.; Martinez, H.; Chaudret, B. InP/ZnS Nanocrystals: Coupling NMR and XPS for Fine Surface and Interface Description. *J. Am. Chem. Soc.* **2012**, *134*, 19701-19708.

(10) Baquero, E. A.; Ojo, W.-S.; Coppel, Y.; Chaudret, B.; Urbaszek, B.; Nayral, C.; Delpech, F. Identifying Short Surface Ligands on Metal Phosphide Quantum Dots. *Phys. Chem. Chem. Phys.* **2016**, *18*, 17330-17334.

(11) Xie, L.; Harris, D. K.; Bawendi, M. G.; Jensen, K. F. Effect of Trace Water on the Growth of Indium Phsophide Quantum Dots. *Chem. Mater.* **2015**, *27*, 5058-5063.

(12) Ramasamy, P.; Kim, B.; Lee, M.-S.; Lee, J.-S. Beneficial Effects of Water in the Colloidal Synthesis of InP/ZnS Core-Shell Quantum Dots for Optoelectronic Applications. *Nanoscale* **2016**, *8*, 17159-17168.

(13) Zherebetskyy, D.; Scheele, M.; Zhang, Y.; Bronstein, N.; Thompson, C.; Britt, D.; Salmeron, M.; Alivisatos, P.; Wang, L.-W. Hydroxylation of the Surface of PbS Nanocrystals Passivated with Oleic Acid. *Science* **2014**, *344*, 1380-1384.

(14) Bertrand, G. H. V.; Polovitsyn, A.; Christodoulou, S.; Khan, A. H.; Moreels, I. Shape Control of Zincblende CdSe Nanoplatelets. *Chem. Commun.* **2016**, *52*, 11975-11978.

(15) Malgras, V.; Nattestad, A.; Yamauchi, Y.; Dou, S. X.; Kim, J. H. The Effect of Surface Passivation on the Structure of Sulphur-Rich PbS Colloidal Quantum Dots for Photovoltaic Application. *Nanoscale* **2015**, *7*, 5706-5711.

(16) Luther, J. M.; Law, M.; Song, Q.; Perkins, C. L.; Beard, M. C.; Nozik, A. J. Structural, Optical, and Electrical Properties of Self-Assembled Films of PbSe Nanocrystals Treated with 1,2-Ethanedithiol. *ACS Nano* **2008**, *2*, 271-280.

(17) The Group 13 Metals Aluminium, Gallium, Indium and Thallium: Chemical Patterns and Peculiarities, Aldridge, S. and Downs A. J. Eds. John Wiley & Sons, **2011**.

(18) Gebhard, M.; Hellwig, M.; Kroll, A.; Rogalla, D.; Winter, M.; Mallick, B.; Ludwig, A.; Wiesing, M.; Wieck, A. D.; Grundmeier, G.; Devi, A. New Amidinate Complexes of Indium(III): Promising CVD Precursors for Transparent and Conductive In_2O_3 Thin Films. *Dalton Trans.* **2017**, *46*, 10220-10231.

(19) McCarthy, R. F.; Weimer, M. S.; Emery, J. D.; Hock, A. S.; Martinson, A. B. F. Oxygen-Free Atomic Layer Deposition of Indium Sulfide. *ACS Appl. Mater. Interf.* **2014**, *6*, 12137-12145.

(20) Tomaselli, M.; Yarger, J. L.; Bruchez, M.; Havlin, R. H.; de Graw, D.; Pines, A.; Alivisatos, A. P. NMR Study of InP Quantum Dots: Surface Structure and Size Effects. *J. Chem. Phys.* **1999**, *110*, 8861-8864.

(21) Lucey, D. W. MacRae, D. J. Furis, M. Sahoo, Y. Cartwright, A. N. Prasad P. N. Monodispersed InP Quantum Dots Prepared by Colloidal Chemistry in a Noncoordinating Solvent. *Chem. Mater.* **2005**, *17*, 3754-3762.

(22) Ryu, E.; Kim, S.; Jang, E.; Jun, S.; Jang, H.; Kim, B.; Kim, S.-W. Step-Wise Synthesis of InP/ZnS Core-Shell Quantum Dots and the Role of Zinc Acetate. *Chem. Mater.* **2009**, *21*, 573-575.

(23) Li, Y.; Pu, C.; Peng X. Surface Activation of Colloidal Indium Phosphide Nanocrystals. *Nano. Res.* **2017**, *10*, 941-958.

(24) Wu, H.; Yang, Y.; Cao, Y. C. Synthesis of Colloidal Uranium-Dioxide Nanocrystals. *J. Am. Chem. Soc.* **2006**, *128*, 16522-16523.

(25) Protiere, M.; Reiss, P. Amine-Induced Growth of an In_2O_3 Shell on Colloidal InP Nanocrystals. *Chem. Commun.* **2007**, 2417-2419.

(26) Bruno, G.; Losurdo, M.; Capezzuto, P. On the Use of H_2 Plasma for the Cleaning and Passivation of InP Substrates. *J. Phys. IV* **1995**, *5*, C5-663-C5-670.

(27) Seager, C. H. In *Semiconductors and Semimetals*; Hydrogenation methods. Jacques, I. P., Noble, M. J., Eds.; Elsevier: **1991**; Vol. 34, pp 17-33.

(28) Tessier, M. D.; Dupont, D.; De Nolf, K.; De Roo, J.; Hens, Z. Economic and Size-Tunable Synthesis of InP/ZnE (E = S, Se) Colloidal Quantum Dots. *Chem. Mater.* **2015**, *27*, 4893-4898.

(29) Peng, X. An Essay on Synthetic Chemistry of Colloidal Nanocrystals. *Nano Res.* **2009**, *2*, 425-447.

(30) Truflandier, L. A.; Del Rosal, I.; Chaudret, B.; Poteau, R.; Gerber, I. C. Where Does Hydrogen Absorb on Ru Nanoparticles? A Powerful Joint 2H MAS-NMR/DFT Approach. *ChemPhysChem.* **2009**, *10*, 2939-2942.

(31) Pery, T.; Pelzer, K.; Buntkowsky, G.; Philippot, K.; Limbach, H.-H.; Chaudret, B. Direct NMR Evidence for the Presence of Mobile Surface Hydrides on Ruthenium Nanoparticles. *ChemPhysChem* **2005**, *6*, 605-607.

(32) Hibbs, D. E.; Hursthouse, M. B.; Jones, C.; Smithies, N. A. Synthesis, Crystal and Molecular Structure of the First Indium Trihydride Complex $[InH_3\{C(N(Pr^i)C_2Me_2N)(Pr^i)\}]$. *Chem. Commun.* **1998**, 869-870.

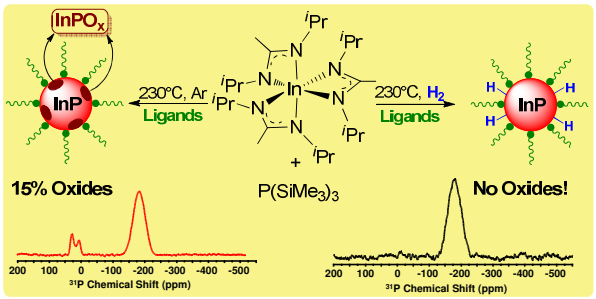
InPO$_x$
InP
230°C, Ar
Ligands
^{i}Pr
^{i}Pr
^{i}Pr
^{i}Pr
^{i}Pr
^{i}Pr
N
N
N
N
N
N
In
+
P(SiMe$_3$)$_3$
230°C, H$_2$
Ligands
H
H
H
H
InP
15% Oxides
No Oxides!
200 100 0 -100 -200 -300 -400 -500
^{31}P Chemical Shift (ppm)
200 100 0 -100 -200 -300 -400 -500
^{31}P Chemical Shift (ppm)